JOURNAL OF THERMOPHYSICS AND HEAT TRANSFER
Vol. 9, No. 1, January–March 1995

Transient Experiments of an Inclined Copper-Water Heat Pipe

Mohamed S. El-Genk,* Lianmin Huang,† and Jean-Michel Tournier†
University of New Mexico, Albuquerque, New Mexico 87131

The effects of inclination angle on the transient operation of a gravity-assisted copper-water heat pipe are investigated experimentally. The inclination angle and the input power are varied from 0 (horizontal) to 90 deg (vertical), and from 520 to 820 W, respectively. The transient vapor and wall temperatures are measured at 11 axial locations along the length of the heat pipe. The heatup and cooldown time constants, although specific to this heat pipe design and experimental setup, are used to assess the effect of the inclination angle at different power input and cooling rates. The experimental data of the transient vapor and wall temperatures and the effective power throughput are also used to benchmark a two-dimensional, heat pipe transient analysis model. The model predictions are in good agreement with experiments.

Nomenclature

$\dot{m}$ = cooling water mass flow rate, g/s
P_e = electric power input, W
P_{cool} = effective power throughput in heat pipe, W
P_{loss} = heat loss through the insulation, W
T = temperature, °C
t = time, s
X = variable in Eqs. (1) and (2), $(T_v - T_{v,o})$ or P_{cool}
θ = inclination angle of heat pipe, deg
τ = time constant, in Eqs. (1) and (2), s

Subscripts
c = cooldown or condenser
h = heatup
o = initial, or beginning of a transient process
ss = steady state
v = vapor
w = wall

Introduction

THE effect of gravity on transient operation of heat pipes is of interest to many space applications such as thermal management, heat rejection radiators, and surface power on the Lunar and Martian surfaces. Many experimental and theoretical studies have been reported on the transient operation of liquid-metal and nonliquid metal heat pipes.[1-11] However, most transient studies on the effect of gravity, or inclination angle, have been applied to thermosiphons.[12,13] Furthermore, transient measurements of not only the wall temperature and the effective power throughput, but also the vapor temperature are needed for benchmarking transient heat pipe models.

Results of several transient experiments of water heat pipes have been published; however, the measurements of the axial distribution of the vapor temperature have been inconclusive.[1,14] Schmalhofer and Faghri[14] have used multiple-point thermocouples to measure the vapor temperature at different axial locations in the vapor region; however, only one temperature measurement was recorded in the evaporator section. Consequently, the actual vapor temperature distribution in the heat pipe during heatup transients could not be deduced from the experimental data. Fox and Thomson[1] have measured the axial and radial vapor temperature distributions in a water heat pipe. At each of 10 axial positions in the heat pipe, they measured the vapor temperature at four radial positions. Because Fox and Thomson's experiments were initiated by changing the cooling conditions and holding the input power constant, the data is of limited use for verifying calculational models during startup transients.

Recently, El-Genk and Huang[3] reported the results of transient experiments using a 600-mm-long, horizontal copper-water heat pipe, having a uniformly heated evaporator section and a convectively cooled condenser section. The transient response of the heat pipe to step changes in input power, at different cooling rates, was investigated. Vapor temperatures were successfully measured at 10 axial locations using a specially designed probe, which was installed along the centerline of the heat pipe. While the experiments of El-Genk and Huang[3] have generated sufficient data for heatup, steady-state, and cooldown transients, which can be used for model verification, they are limited to either a horizontal configuration or a zero gravity condition. The steady-state performance of a gravity-assisted heat pipe is usually enhanced due to improved liquid flow in the wick region. However, during transient operation such as startup or changes in input power or cooling rate, determining the effect of gravity on transient operation of heat pipes is of interest to space applications.

The objective of this article is to extend the work of El-Genk and Huang[3] to 1) experimentally investigate the effect of the inclination angle on the transient operation of a 900-mm-long, copper-water heat pipe subject to step changes in input power, at different cooling rates; and 2) use measured vapor and wall temperatures and the effective power throughput to benchmark a two-dimensional heat pipe transient analysis model (HPTAM).[10,11]

Experimental Procedures

Figures 1a and 1b present a schematic diagram and a photograph of the experimental setup, respectively. Figures 2a and 2b show longitudinal cross section of the heat pipe and a photograph of the disassembled heat pipe, respectively. The copper-water heat pipe, 17.3 mm i.d. and 19.1 mm o.d., has two layers of a 150-mesh copper screen wick. The length of the evaporator, adiabatic, and condenser sections is 600, 90, and 200 mm, respectively. The evaporator section is much longer than the condenser section in order to allow accurate measurements of the axial vapor temperature distribution, which are needed for model verification. The vapor temperature is measured along the centerline of the heat pipe using a special probe made of a thin wall, brass tube (3.2 mm o.d.), and instrumented with 11 K-type thermocouples. The ther-

Received Aug. 30, 1993; revision received Feb. 8, 1994; accepted for publication June 14, 1994.

*Professor and Director, Department of Chemical and Nuclear Engineering, Institute for Space and Nuclear Power Studies.

†Ph.D. Candidate, Department of Chemical and Nuclear Engineering, Institute for Space and Nuclear Power Studies.

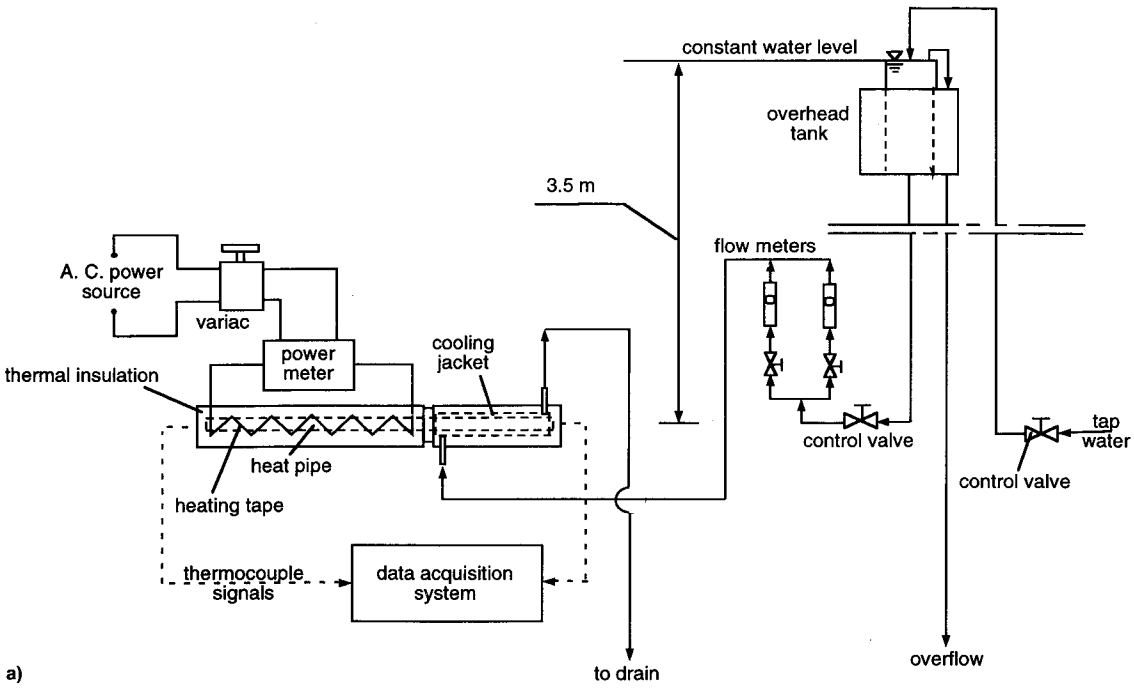

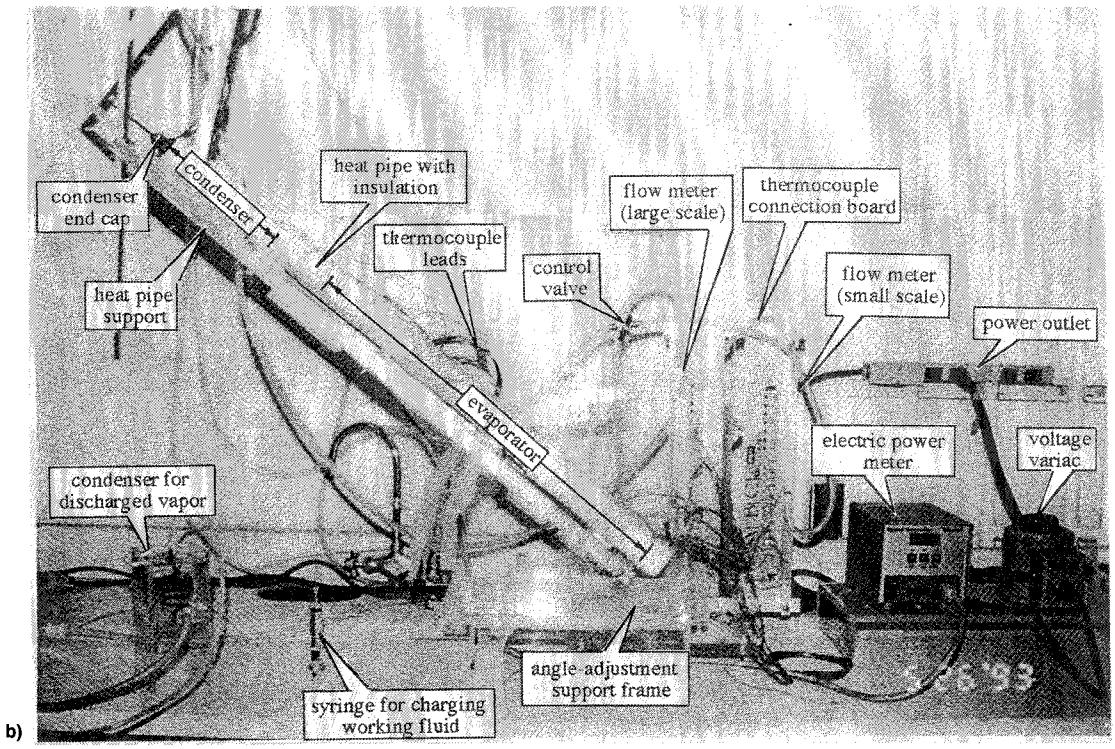

Fig. 1 a) Schematic diagram and b) a photograph of the experimental setup.

mocouples, $T_{v1}-T_{v11}$, in the probe are used to measure the vapor temperature at different axial locations of the heat pipe. These thermocouples are inserted into the probe shell and pulled out through tiny holes along the probe wall. The thermocouples are then soldered on the outer surface of the probe wall, but their ends are kept about 0.1 mm above the probe wall surface to directly measure the vapor temperature (Fig. 3). An additional 11 thermocouples are attached to the outer surface of the heat pipe wall to measure its temperature at the same axial locations as the vapor temperature thermocouples (Fig. 2a).

The evaporator section is uniformly heated using a flexible ac electrical tape, and the condenser section is convectively cooled with water. An overhead tank is used to stabilize the water flow rate to the condenser cooling jacket, and the water inlet and exit temperatures are measured using K-type thermocouples. These measurements are used to determine the effective power throughput in the heat pipe during the transient.[3] The evaporator section's ceramic fiber-type insulation is instrumented with K-type thermocouples to determine the surface heat losses by natural convection to ambient. The electric power input to the heater of the evaporator section is measured directly using a power meter and controlled by a variable resistance variac.

The input electrical power is varied from 520 to 820 W, and the water flow rate in the condenser cooling jacket is varied from 2 to 22 g/s. The transient data from the experiments is used to determine the heatup and cooldown time

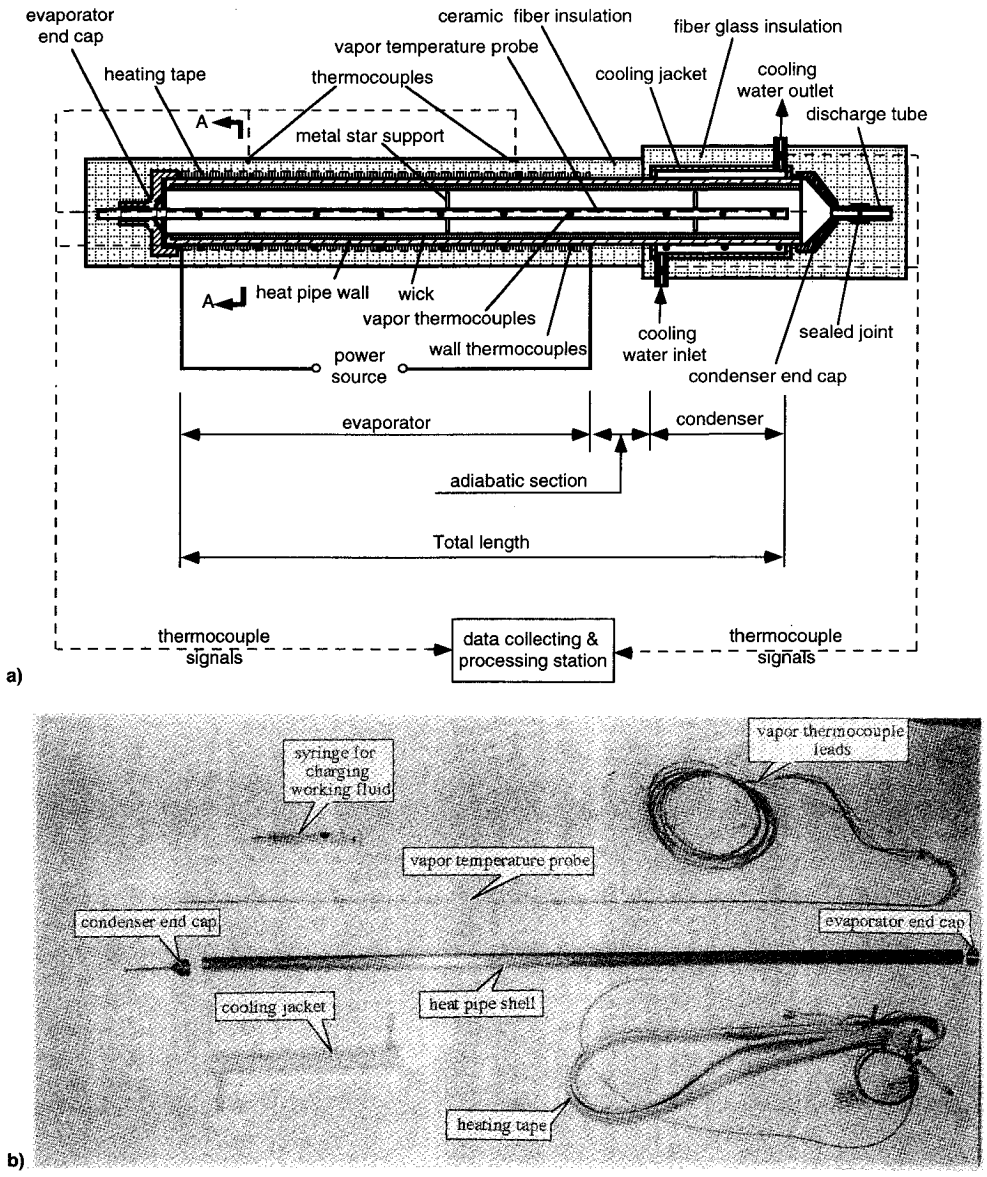

Fig. 2 a) Longitudinal cross section of the copper-water heat pipe and b) a photograph showing the parts of the disassembled heat pipe.

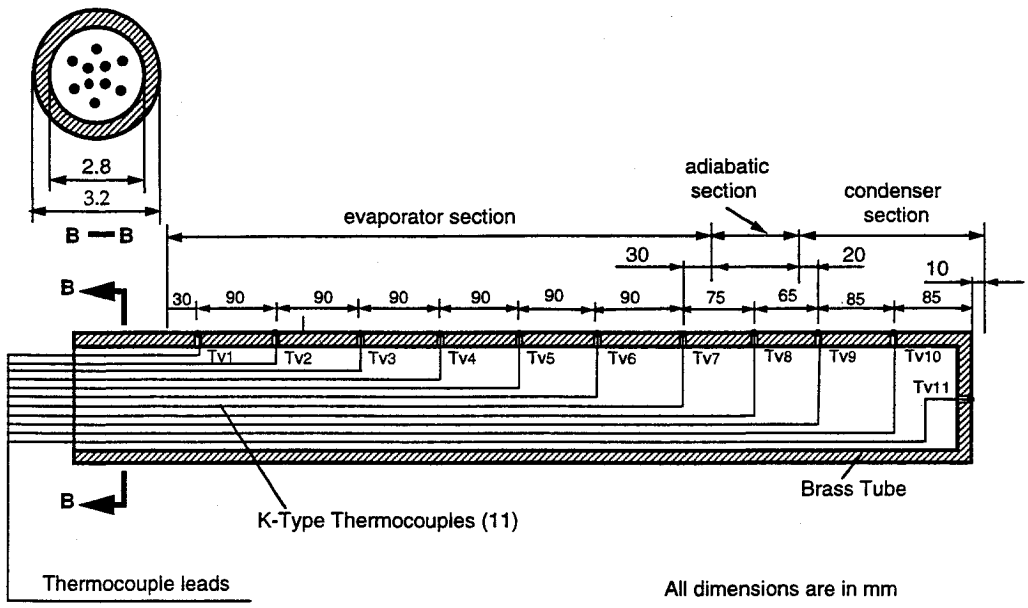

Fig. 3 Longitudinal cross section of the vapor temperature probe.

constants for both the vapor temperature and the effective power throughput, as functions of the inclination angle, input power, and cooling water flow rate. The accuracy of the measurements is about ±0.4 K for temperatures, using calibrated thermocouples, ±2% for electric power input, ±2% for the cooling water flow rate, and ±0.5 deg for the inclination angle. Based on these measurement errors, there is an uncertainty of about ±4% in P_{cool}, ±3.5% in P_{loss} in the evaporator section by natural convection to ambient.[15] The above uncertainty in the heat loss rate includes that of the experimental correlation for calculating natural convection heat transfer (±15%).

Before each experiment, the inclination angle and the water flow in the cooling jacket are adjusted to the desired values. The instrumented heat pipe is mounted on a Plexiglas® frame with a special arrangement for adjusting the inclination angle. The heatup transient is initiated by increasing the electric power to the heating tape in the evaporator section in a step function, from zero to the required value. The transient continues until steady state is reached. Then, the cooldown transient is initiated by reducing electric power to the evaporator section in a step function to zero, but keeping the cooling water flow rate unchanged. After the heat pipe and the insulation cooldown to almost room temperature, another transient experiment is initiated.

Results and Discussion

To verify the setup and experimental measurements, a steady-state heat balance is performed. The electric power input to the evaporator section P_e is compared with the sum of the calculated heat loss rate from the insulation surface by natural convection P_{loss}, and P_{cool} (or the heat rejection in the condenser section). The effective power throughput is determined from the heat balance in the cooling jacket of the condenser section, and the heat loss rate from the outer surface of the insulation shell is determined from the measured insulation temperature and the heat transfer coefficient using a natural convection correlation.[16] In this correlation, the air properties are evaluated at the mean film temperature.[3] Figure 4 presents such a comparison for 10-deg inclination. As shown, the sum of P_{cool} and P_{loss} is within less than 5% of the electric power input at steady state.

Axial Temperature Distribution During Transient

Figure 5 presents the measured wall and vapor temperatures along the heat pipe for an inclination angle of 10 deg. Figure 5c indicates that after about 88 s, the vapor temperature is almost uniform along the heat pipe. The wall temperature is also uniform in the evaporator section, but increases with distance in the condenser section. It is lowest at the beginning of the condenser, where the water enters the cooling jacket, and highest at the end of the condenser where water exits the jacket.

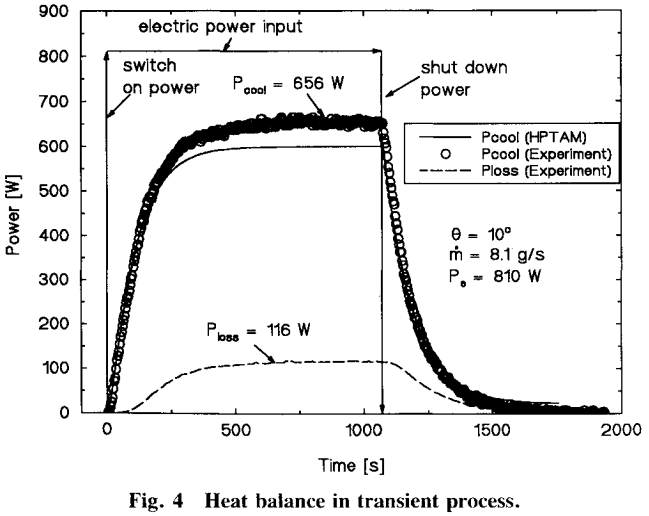

Fig. 4 Heat balance in transient process.

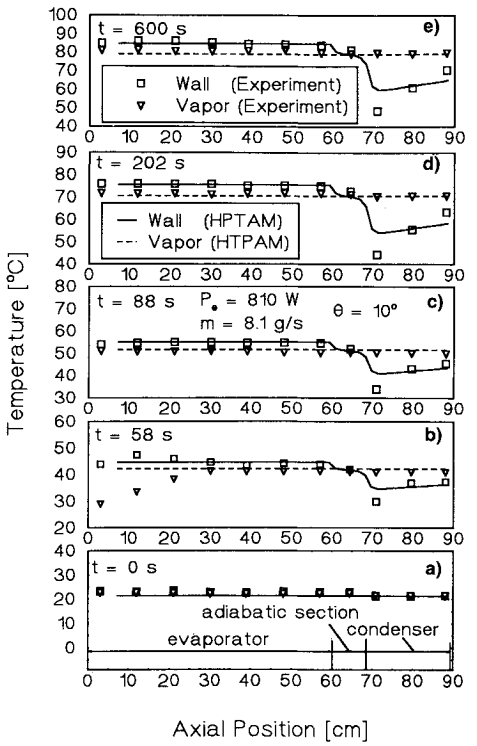

Fig. 5 Transient vapor and wall temperature distributions and comparison with HPTAM.

At the beginning of the transient experiments, the heat pipe temperature is uniform and equal to about 22°C. During the transient, the fraction of the electric power input to the heater in the evaporator section, which is transported by the heat pipe working fluid, increases causing the wall and the vapor temperatures to increase. As shown in Fig. 5b, the wall temperature in the evaporator section is almost uniform, except at the beginning of the evaporator section, where it is slightly lower due to the heat losses to the copper end cap and probe. As the heat pipe wall heats up, and since the evaporator end is thermally insulated, end heat loss becomes negligible, as indicated by the uniformity of the wall temperature distributions in the evaporator section in Figs. 5c–5e. The axial conduction in the heat pipe wall causes its temperature near to the adiabatic section to be slightly lower.

The results in Fig. 5 indicate that the vapor temperature is almost uniform along the entire length of the heat pipe, except at the beginning of the transient. As Fig. 5b shows, the three thermocouples close to the evaporator end measure lower temperature than the other eight thermocouples attached to the vapor temperature probe (Fig. 3). The response of these thermocouples could have been affected by the inclination angle of the heat pipe. Because the vapor temperature probe brass tube functions as a fin during the cooldown phase of the heat pipe, vapor partially condenses on the surface of the probe, forming a thin liquid film. When the heat pipe is heated up again in the horizontal position, this film drains off the upper surface of the probe, where the vapor thermocouples are attached to the wall of the probe. Consequently, all probe thermocouples measure the same transient change in the vapor temperature (Fig. 6a).

When the heat pipe is operated in an inclined position, the condensate film on the vapor probe drains down to the evaporator end and covers the lower thermocouples (T_{v1}, T_{v2}, and/or T_{v3}). These thermocouples are located 30, 120, and 210 mm from the evaporator end, respectively. Consequently, when the heatup transient is initiated, these thermocouples measure lower temperatures until the film evaporates. As the

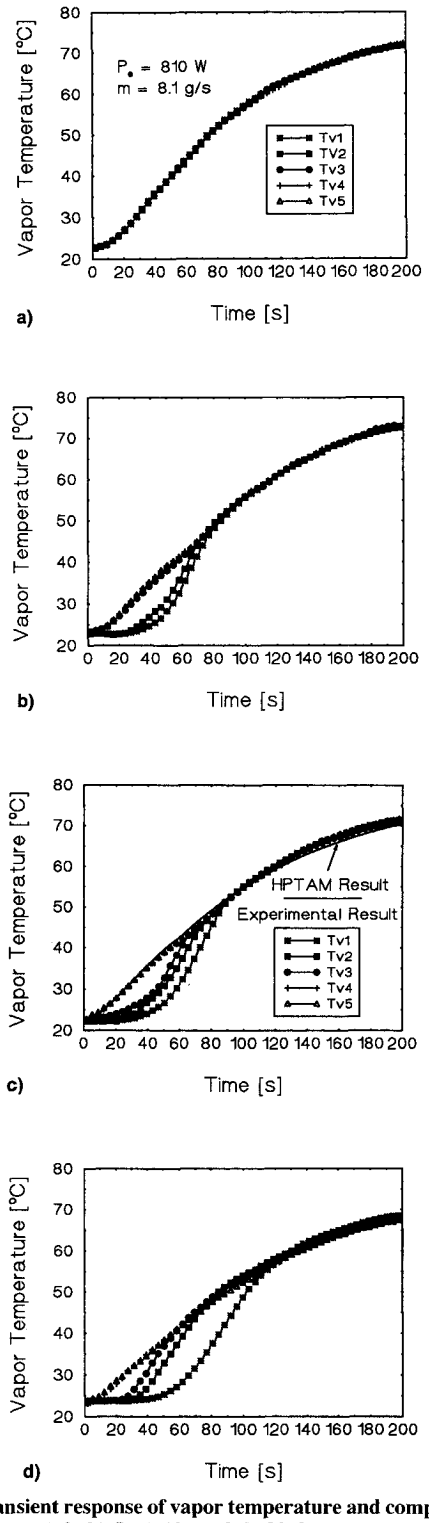

Fig. 6 Transient response of vapor temperature and comparison with HPTAM. θ = a) 0, b) 5, c) 10, and d) 90 deg.

film evaporates, the thermocouples (T_{v1}, T_{v2}, then T_{v3}) senses higher temperatures and eventually record the same temperature as the other thermocouples located at higher position on the probe. In the vertical position, it takes approximately 2 min to evaporate the water film, and only about 90 and 75 s for θ = 10 and 5 deg, respectively (Figs. 6b–6d). After approximately 200 s into the heatup transient, the vapor temperatures along the heat pipe are within less than 5% of each other, regardless of the inclination angle. As a result, early nonuniformity in the measured vapor temperature minimally affects the heat pipe transient response.

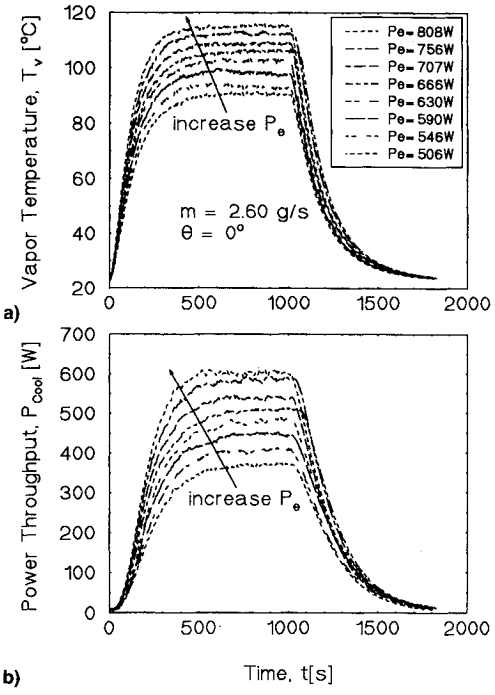

Fig. 7 Transient response of the heat pipe at different heating power: a) vapor temperature and b) power throughput.

Effect of Power Input

Figures 7a and 7b present typical measurements of the vapor temperature and the effective power throughput during both heatup and cooldown transients. As these figures indicate, increasing the input electric power in the evaporator section increases the steady-state values of both P_{cool} and T_v. In all cases, the cooldown process is initiated by a step function drop in the electric power input to zero at approximately 1000 s.

Heat Pipe Time Constants

To determine the heatup and cooldown time constants for either T_v or P_{cool}, the experimental data is fitted using an exponential relation:

$$X(t) = X_{ss}[1 - e^{-(t-t_o)/\tau_h}] \quad \text{(during heatup)} \qquad (1)$$

$$X(t) = X_{ss}e^{-(t-t_o)/\tau_c} \quad \text{(during cooldown)} \qquad (2)$$

In Eqs. (1) and (2), X_{ss} is the steady-state value of X. In these equations, t_o is an arbitrary time for initiating the transient, and τ is the time constant that characterizes the transient process being investigated.

As El-Genk and Huang[3] have indicated, the heatup and cooldown time constants for a heat pipe can be expressed as the ratio of the steady-state values of the measured variable divided by its slope at the beginning of the transient, which are determined from the experiments. As shown in Figs. 8a and 8b, the inclination angle minimally affects the time constants of the heat pipe. However, increasing the cooling water flow rate lowers the time constants for both T_v and P_{cool}. Unlike the inclination angle, the cooling water flow rate for the heat pipe strongly affects the time constants of P_{cool} and T_v during both the heatup and cooldown transients. As Figs. 9a and 9b show, increasing the coolant flow rate up to about 10 g/s causes the heat pipe time constants to decrease rapidly (i.e., faster response). Higher flow rates, however, insignificantly affects the heat pipe time constants. Figures 9a and 9b also show that the inclination angle of the heat pipe minimally affects the time constants of the heat pipe. The heatup and cooldown time constants for the effective power throughput are generally higher than that for the vapor temperature,

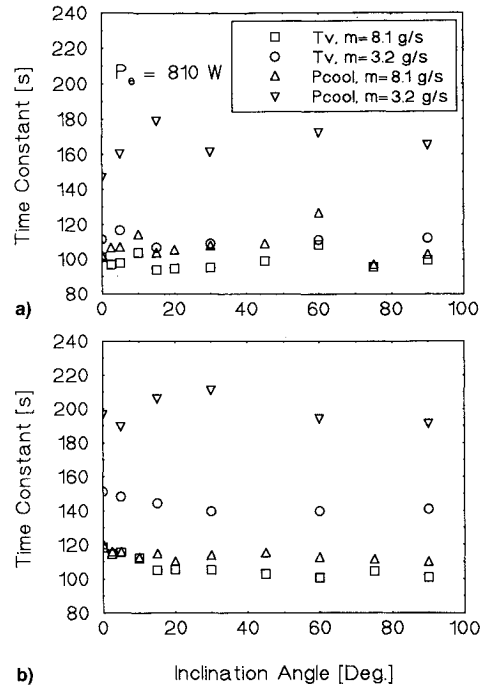

Fig. 8 Effect of the inclination angle on the time constant: a) heatup and b) cooldown process.

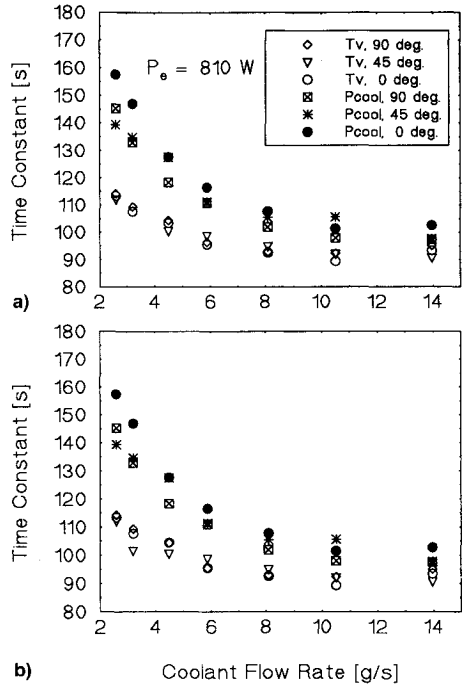

Fig. 9 Effect of cooling rate on the time constant: a) heatup and b) cooldown process.

particularly at low coolant flow rate in the condenser section. The transient results in Figs. 8 and 9, although specific to this heat pipe design and experimental setup, provide good comparison of the effects of the inclination angle and both the heating and cooling rates.

Figures 10a and 10b indicate that increasing P_e lowers the time constants. However, the effect of the electric power input to the evaporator on the P_{cool} time constants is more pronounced than on the T_v time constants. These figures once again show that heat pipe time constants decrease rapidly as the cooling water flow rate increases up to 10 g/s, and at higher flow rates, the effect on time constants becomes insignificant. For values between 2.6–10 g/s, the heat pipe time constants

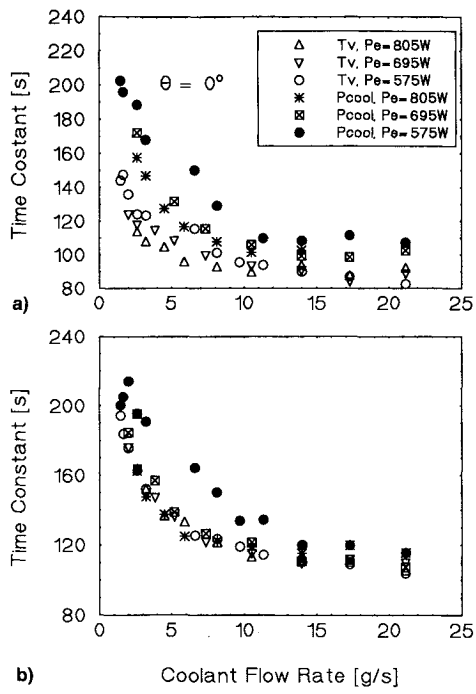

Fig. 10 Effect of heating power on the time constant: a) heatup and b) cooldown process.

are more sensitive to changing P_e than at lower or higher values. In general, increasing P_e lowers the time constants for T_v and P_{cool} (i.e., faster transient response of the heat pipe).

Heat Pipe Model Description

Many transient heat pipe models have been reported; however, they incorporate various simplifying assumptions. Bowman et al.[4] and others have modeled the heat pipe as a single vapor region. Other investigators[5,6] incorporated the vapor, liquid-wick, and wall regions in a single calculation domain. Jang et al.[5] modeled the heat pipe startup from the frozen state, but neglected the liquid flow in the wick. Faghri and Buchko[6] modeled the steady-state operation of fully-thawed heat pipes and included the liquid flow in the wick. These models,[5,6] however, neglected the hydrodynamic coupling between the liquid and vapor regions. Seo and El-Genk[8] modeled the vapor, liquid-wick, and wall regions in a single calculation domain, and incorporated thermal and hydrodynamic couplings of the vapor and liquid phases. These couplings are essential in order to correctly predict the capillary limit and dryout conditions during transient operation of the heat pipe. Seo and El-Genk[8] also used a quasi-steady-state, one-dimensional approximation to simulate the vapor flow. However, at startup, when a heat pipe is operating at low vapor density, large radial temperature gradients may develop in the wall, liquid-wick, and vapor regions, requiring a two-dimensional transient modeling approach. Furthermore, since working fluids such as water and liquid-metals have high thermal expansion coefficients, liquid compressibility should be considered to account for potential pooling of the working fluid at the end of the condenser region during startup transients. To the best of the authors' knowledge, none of the existing heat pipe models has the capability of predicting such liquid pooling.

HPTAM, a fully two-dimensional code, was developed to overcome the limitations of existing models.[10] For example, HPTAM couples the liquid and vapor phases, and unlike previous models, solves for the radius of curvature of the liquid meniscus at the liquid-vapor (L-V) interface and models liquid pooling phenomena during startup and shutdown transients.

The model divides the cylindrical heat pipe into three radial regions: wall, liquid-wick, and vapor regions, employs the

complete form of the compressible flow equations in the vapor region, and uses the Brinkman-Forchheimer-extended Darcy's equations to predict the liquid flow in the wick. The wick is either an annular wire-screened mesh or a homogeneous porous medium, which preserve the circular symmetry in the cross section of the pipe. The evaporation/condensation rates at the L-V interface are obtained from the kinetic theory of gases.

Because HPTAM is a fully two-dimensional model, it can easily incorporate the momentum and enthalpy jump conditions at the L-V interface. The model uses the capillary relationship (the radial momentum jump condition) to relate the phasic pressures, and the radius of curvature of the liquid meniscus at the L-V interface is geometrically related to the vapor volume fraction in the wick. More details on the governing equations and the physical model in HPTAM can be found in Tournier and El-Genk.[10]

The governing equations and boundary conditions in HPTAM are discretized using the volume integration method of Patankar, and the numerical scheme is developed using the well-known Eulerian staggered-grid. The liquid and vapor velocities are determined at the cell boundaries, whereas the other quantities, such as pressures and enthalpies, are evaluated at the cell center. The numerical solution is obtained using a segregated solution technique similar to the SIMPLEC algorithm, with special treatments at the L-V interface. In the first step of the numerical algorithm, the pressure gradient in the conservative forms of the momentum equations is discretized implicitly, and the off-diagonal velocity corrections appearing in the diffusion/convection terms are equated to the diagonal velocity correction. The evaporation-condensation rates are linearized in terms of the vapor pressures using the kinetic theory of gases. By eliminating the advanced-time mass fluxes appearing in the mass balance equation and considering the pressure variation with the density, the continuity equation is reduced to the Poisson equation, which is then solved for the pressure field. During this predictor step, liquid and vapor volumes around the L-V interface are treated as functions of the wick void fractions. These void fractions are geometrically related to the cosines of the contact angles. The latter are implicitly related to the liquid and vapor pressures at the L-V interface through the capillary relationship. The densities and radii of curvature of the liquid meniscus for the advanced time are then obtained, with the temporary new-iteration pressures and mass fluxes.

HPTAM handles the liquid-pooling phenomenon described above as follows. When a convex liquid meniscus occurs somewhere along the heat pipe, the interface is assumed flat at this particular location, and the capillary relationship is used to calculate the pressure in the liquid cell next to the diphasic interface. Then, using the mass balance in this cell, the mass of the excess liquid pooling is determined. This mass is then transported into the next interfacial liquid cell. Once the wet point reaches the end of the condenser, the liquid forms a pool in the vapor core region. More details on the numerical solution are available elsewhere.[11]

Comparison of Model with Experiments

The model predictions are compared with the transient results of the 10-deg inclination water heat pipe experiment in Figs. 4–6. Because the water flow rate in the cooling jacket is relatively small (8.1 g/s), a transient one-dimensional water jacket submodel is developed and thermally coupled to the condenser wall to calculate the axial distribution of the coolant bulk temperature in the jacket. At steady state, the convective heat transfer coefficient in the jacket is determined from the experiment to be 1600 W/m^2.K; this value was used in the model for the whole transient simulation. The wick effective pore radius, porosity, and permeability are taken as 54 μm, 0.9, and 1.5 $\times$ 10^{-9} m^2, respectively. The effective thickness of the liquid-wick region was taken as 0.60 mm. The thermal conductivity of the liquid-wick region is calculated assuming a distributed-cylinders configuration having an effective porosity of 0.5. The accommodation coefficient for water evaporation is taken as 0.1, which accounts for the fact that not every vapor molecule that hits the surface condenses, and not every liquid molecule that evaporates remains in the vapor. The average vapor void fraction in the wick at startup is calculated based on the water charge in the experimental heat pipe, and is equal to 0.15. Before initiating the heatup transient calculations, the coupled continuity and momentum equations in HPTAM are solved for the liquid and vapor pressure distributions and the vapor pore void fraction axial profile due to the inclination angle. These distributions are then used to initiate the transient heatup calculations.

To account for the effective heat input in the evaporator section, calculations are performed with the measured transient wall temperatures along the evaporator section. Figure 4 compares the calculated transient response of the effective power throughput, determined from the heat balance in the cooling jacket, with experimental data. As Fig. 4 shows, the comparison is quite good for the heatup and cooldown transients. However, the calculated steady-state power throughput (600 W) is 9% lower than the experimental value of 650 W. This slight underprediction of the power throughput by the model is due to the uncertainty in determining the exact spacing between the wall and the wick structure along the experimental heat pipe.

Figure 5 compares the calculated wall and vapor temperatures along the heat pipe with those measured at different times during the transient (0, 58, 88, 202, and 600 s). All temperature calculations in the heat pipe are initialized at room temperature of 21.3°C (Fig. 5a). Because the model assumes that both ends of the heat pipe are insulated, the evaporator end effects shown in Fig. 5b are not accounted for numerically. Also, condensation on the vapor probe and liquid film hydrodynamics are not modeled. Figure 5 shows good agreement between measured and calculated wall and vapor temperatures. At steady state, the calculated vapor temperature (79°C) is only 2.0 K lower than that measured (Fig. 5e). The difference between calculated and measured wall temperature in the condenser section is attributed to the fact that an axially uniform convective heat transfer coefficient is used along the cooling jacket. Also, the condensation rate at the L-V interface decreases along the condenser, due to the increase in the cooling water temperature. As shown in Fig. 6c, the calculated transient vapor temperature compares very well with experimental measurements during the first 200 s of the heatup transient; this good agreement is also true for the full heatup and cooldown transients. Such good agreement between calculation and transient experimental data verifies the soundness of the system of equations and the modeling approach used in HPTAM.

Summary and Conclusions

Experiments are performed to investigate the transient response of an inclined, gravity-assisted, copper-water heat pipe to step changes in input power, at different cooling rates. Direct measurements of the axial vapor and wall temperature distributions are obtained along the entire length of the heat pipe. The heatup and cooldown time constants, although specific to this heat pipe design and experimental setup, are used together with the measured vapor and wall temperatures to assess the effect of the inclination angle at different power inputs and cooling rates. The experimental results are also used to benchmark a two-dimensional, HPTAM. The model predictions of the vapor and wall temperatures and the effective power throughput for a 10-deg inclination are in good agreement with data during the heatup, steady-state, and cooldown processes.

Results indicate that although the heat pipe time constants are not significantly affected by the inclination angle, increas-

ing the cooling water flow rate up to 10 g/s shortens the response of the heat pipe by lowering the time constant. At higher water flow rates, the change in the heat pipe time constants with inclination angle is relatively small. Increasing the electric power input to the evaporator lowers P_{cool} time constants, and to a lesser extent the time constants of T_v. The results also show that the inclination angle insignificantly affects the transient response of the heat pipe or its steady-state operation.

References

[1]Fox, R. D., and Thomson, W. J., "Internal Measurements of a Water Heat Pipe," *Proceedings of the Intersociety Energy Conversion Engineering Conference* (Las Vegas, NV), 1970, pp. 7-72–7-76 (IECEC-709106).

[2]Faghri, A., Buchko, M., and Cao, Y., "A Study of High Temperature Heat Pipes with Multiple Heat Sources and Sinks (Part I: Experimental Methodology and Frozen Startup Profiles)," *Journal of Heat Transfer*, Vol. 113, No. 4, 1991, pp. 1003–1009.

[3]El-Genk, M. S., and Huang, L., "An Experimental Investigation of a Water Heat Pipe," *International Journal of Heat and Mass Transfer*, Vol. 36, No. 15, 1993, pp. 3823–3830.

[4]Bowman, W. J., McClure, W. B., Towne, M. C., and Rizzetta, D. P., "Transient Heat-Pipe Modeling, Paper 2," AIAA Paper 90-0061, Jan. 1990.

[5]Jang, H. J., Faghri, A., Chang, W. S., and Mahefkey, E. T., "Mathematical Modeling and Analysis of Heat Pipe Startup from the Frozen State," *Journal of Heat Transfer*, Vol. 112, 1990, pp. 586–594.

[6]Faghri, A., and Buchko, M., "Experimental and Numerical Analysis of Low-Temperature Heat Pipes with Multiple Heat Sources," *Journal of Heat Transfer*, Vol. 113, No. 3, 1991, pp. 728–734.

[7]Colwell, G. T., and Modlin, J. M., "Mathematical Heat Pipe Models," *Proceedings of the 8th International Heat Pipe Conference*, edited by M. Tongze, International Academic Publisher, Beijing, China, 1992, pp. 89–93.

[8]Seo, J. T., and El-Genk, M. S., "A Transient Model for Liquid Metal Heat Pipes," *Space Nuclear Power Systems 1988*, edited by M. S. El-Genk and M. D. Hoover, Vol. IX, Orbit Book Co., Malabar, FL, 1989, pp. 405–418.

[9]El-Genk, M. S., and Seo, J. T., "A Study of the SP-100 Radiator Heat Pipes Response to External Thermal Exposure," *Journal of Propulsion and Power*, Vol. 6, No. 1, 1990, pp. 69–77.

[10]Tournier, J.-M., and El-Genk, M. S., "A Heat Pipe Transient Analysis Model," *International Journal of Heat and Mass Transfer*, Vol. 37, No. 5, 1994, pp. 753–762.

[11]Tournier, J.-M., and El-Genk, M. S., "A Segregated Solution Technique for Simulating the Transient Operation of Heat Pipes," *Journal of Numerical Heat Transfer*, Pt. B: Fundamentals, Vol. 25, 1994, pp. 331–355.

[12]Braven, K., and Den, R., "Two-Phase Heat Transfer in Thermosiphon Evacuated-Tube Solar Collectors," *Journal of Solar Energy Engineering*, Vol. 111, No. 4, 1989, pp. 292–297.

[13]Maezawa, S., Gi, K., and Matsumura, S., "Laminar Film Condensation on Inclined Two-Phase Closed Thermosiphon," *Proceedings of the 8th International Heat Pipe Conference*, edited by M. Tongze, International Academic Publisher, Beijing, China, 1992, pp. 214–219.

[14]Schmalhofer, J., and Faghri, A., "A Study of Circumferentially Heated and Block-Heated Heat Pipes (Part I: Experimental Analysis and Generalized Analytical Prediction of Capillary Limits)," American Society of Mechanical Engineers Annual Winter Meeting, Atlanta, GA, Dec. 1991.

[15]Kline, M., and McClintock, F. A., "Describing Uncertainties in Single-Sample Experiments," *Mechanical Engineering*, Jan. 3–8, 1953.

[16]Karlekar, B. V., and Desmond, R. M., "Engineering Heat Transfer," West Publishing Co., New York, 1977, p. 444.